

# Polymer-Thread-Based Fully Textile Capacitive Sensor Embroidered on a Protective Face Mask for Humidity Detection

Ankita Sinha,<sup>\*,‡</sup> Adrian K. Stavrakis,<sup>‡</sup> Mitar Simić, and Goran M. StojanovićCite This: *ACS Omega* 2022, 7, 44928–44938

Read Online

ACCESS |



Metrics &amp; More

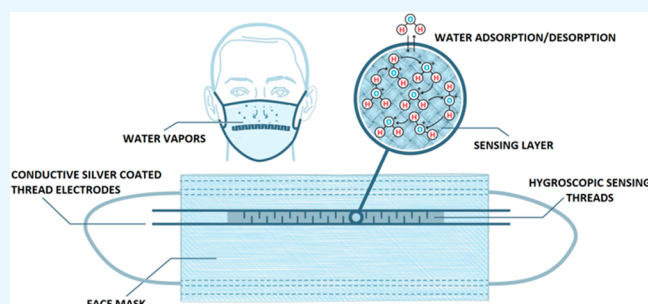


Article Recommendations



Supporting Information

**ABSTRACT:** The COVID-19 pandemic has created a situation where wearing personal protective masks is a must for every human being and introduced them as a part of everyday life. This work demonstrates a new functionality embedded in single-use face masks through an embroidered humidity sensor. The design of the face mask humidity sensor is comprised of interdigitated electrodes made of polyamide-based conductive threads and common polyester threads which act as a dielectric sensing layer embroidered between them. Therefore, the embroidered sensor acts as a capacitor, the performance of which was studied in increasing humidity conditions in the frequency range from 1 Hz to 100 kHz. The moisture adsorbed by sensitive hygroscopic polyester threads altered their dielectric and permittivity properties which were detected by the change in capacitance values of the face mask sensors at different relative humidity (RH) levels. The calculated limit of detection (LOD) values for the two proposed sensors at different frequencies (1, 10, and 100 kHz) were found in the range from 11.46% RH–27.41% RH and 29.79% RH–38.65% RH. The tested sensors showed good repeatability and stability under different humidity conditions over a period of 80 min. By employing direct embroidery of silver-coated polyamide conductive threads and moisture-sensitive polyester threads onto the face mask, the present work exploits the application of polymer-based textile materials in developing novel stretchable sensing devices toward e-textile applications.



## 1. INTRODUCTION

Mask wearing can be effective in the containment of communicable diseases and has thus become a new normal in many societies since the COVID-19 pandemic. Face masks are also needed in all surgical wards and dentist offices as well as in cold storage working environments. For now, masks are used only for protection, and there is a need to breathe new life into face masks, in terms of enhancing their functionality to detect different parameters or biomarkers. Bearing in mind that our exhalation on a daily level contains around 0.5 kg of water, it is interesting to embed humidity-sensing functionality into protective face masks. A substantial control of humidity levels is crucial for many industrial applications such as agriculture, medicine, and weather forecasting.<sup>1,2</sup> With the development of wearable and electronic sensors,<sup>3,4</sup> it has now become possible to detect humidity related to the human body such as during respiration, speech, moisture on the skin, and baby diaper monitoring.<sup>5</sup> Though there have been significant efforts reported, many challenges still exist in this field. Water molecules are a major part of human breath, which has an impact on the relative humidity (RH) around our nose and mouth during respiration. In essence, human breath is reported to be nearly saturated with water (>95%) together with nitrogen, oxygen, carbon dioxide, inert gases, and other disease biomarkers such as acetone, ammonia, isoprene, ethanol, etc. in parts per trillion (ppt) and parts per million (ppm)

concentrations.<sup>6</sup> Deviated levels of these breath biomarkers in the body from their standard values can lead to an early level of detection of concerning anomalies in the human body. Thus, detection of human breath and the humidity which arises during respiration is important for early disease monitoring.

Humidity is generally expressed in terms of relative humidity (RH) which is defined as the ratio of the partial pressure of the water vapors present in air to the saturated amount of vapors in air at a given temperature. In common terms, water vapor can be considered as a ubiquitous gas in the atmosphere, which even in trace amounts changes the properties of the medium. Thus, accurate detection of water vapor is highly essential for multiple applications.<sup>7</sup> To address the widespread demand for precise humidity measurement, recent research efforts have aimed to explore novel sensor designs that involve new sensing materials, cost-effective fabrication methods, appropriate flexible substrates, and their easy integration to readout electronics. The advent of the current era of stretchable

Received: August 11, 2022  
Accepted: October 28, 2022  
Published: December 2, 2022



Table 1. Capacitive Humidity Sensors of Different Components and Configurations

Substrate	Humidity sensing material	Fabrication method	% RH range	Ref
Copper wire	Yarn	Mechanical wrapping	6–90	8
Paper	Silver ink	Inkjet printing	40–90	9
Polyimide	Silver ink	Lithography, Inkjet printing	10–70	10
Textile fabric	MIL-96(Al) Metal Organic Framework (MOF)	Langmuir–Blodgett	3.7–90	11
Polyimide	Cellulose acetate butyrate (CAB)	Photolithography, Inkjet printing	25–85	16
Polyester textile	Polydimethylsiloxane–calcium chloride (PDMS-CaCl <sub>2</sub> )	Screen printing	30–60	21
Polyethylene terephthalate	Nb <sub>2</sub> CT <sub>x</sub> MXene-sodium alginate	Electrospinning	11–97	39
Glass/polyethylene terephthalate	Wood-derived nanocellulose paper	Chemical	7–94	40
Epoxy	Indium oxide–graphene oxide (In <sub>2</sub> O <sub>3</sub> -GO)	Chemical	11–97	41
Polyethylene terephthalate	Indium tin oxide–aluminum oxide (ITO-Al <sub>2</sub> O <sub>3</sub> )	Screen printing	5–95	42
Glass	Carbon nanotube-nickel phthalocyanine-poly-N-epoxypropylcarbazole	Chemical	30–90	43
Polyimide	Graphene oxide-polydiallyldimethylammonium chloride (GO-PDDA)	Chemical	11–97	44
Polyimide	Molybdenum disulfide–tin oxide (MoS <sub>2</sub> -SnO <sub>2</sub> )	Chemical	11–97	45
Glass	Keratin–graphene oxide, keratin–carbon fiber	Chemical	16–92	46
Nonwoven polypropylene face mask	Polyester threads	Embroidery	28–78, 36–74	This work

sensors has been expedited by novel developments and innovations in textile electronics and their possible applications for real-time sensing.<sup>1,7</sup> With respect to the device design, generally a humidity sensor is composed of a sensing layer onto a suitable substrate with electrodes for physical interfacing and transduction. The sensors fabricated with appropriate water-sensitive materials, digitized electrode patterns, and stretchable substrates showcase high performance with respect to linearity, sensitivity, reproducibility, and hysteresis.<sup>8,9</sup> Humidity sensors are typically classified into capacitive and resistive types based on their sensing mechanisms.

In humidity sensors, sensitive sensing materials are highly susceptible to adsorption and desorption of water vapors which impacts their dielectric properties, thereby causing changes in capacitance and resistance values and producing different response characteristics. Recently, textile materials have attracted immense attention as sensing materials and as potential substrates in prototyping novel humidity sensors because of their natural abundance, low cost, flexibility, zero toxicity, and biocompatibility over their chemical counterparts. So far, significant efforts have been made to develop different textile-based capacitive<sup>10,11</sup> and resistive<sup>12–15</sup> humidity sensors. The basic methodology recently adopted for fabricating textile sensors is commonly based on weaving<sup>16,17</sup> and sewing<sup>18</sup> techniques. Moreover, coating (e.g., Langmuir–Blodgett, drop coating, spin coating) and printing methods are also reported involving polyimide, polydimethyl sulfoxide, carbon nanomaterials, or ceramic materials as humidity-sensitive materials to textile substrates.<sup>10,11,13,14,19,20</sup> Though these approaches demonstrate significant progress toward developing textile-based humidity sensors, there are several challenges during their fabrication processes, for example, limited durability of sensors prepared by printing and coating methods,<sup>1,8</sup> damage to the surface of the sensing layer, and a decrease of the sensor sensitivity towards detecting water molecules. The state-of-the-art of humidity monitoring has evolved in recent times. Humidity sensors on textile substrates can be utilized in promising wearable applications in current times to monitor various biological parameters such as human water metabolism, breathing, and sweating patterns.<sup>8</sup> However,

it is difficult for conventional hygroscopic polymers, porous silicon, aluminum oxide, or graphene materials to be assembled on textile surfaces as they get deformed during humidity measurements.<sup>21</sup> Therefore, currently the most demanding task in creating a textile-based humidity sensor is its facile and robust fabrication using appropriate sensing materials which have high sensitivity towards water.

Considering the challenges in fabricating textile-based humidity sensors, the present paper reports an embroidered capacitive humidity sensor with appropriately selected polymer-based fiber yarns. Modern embroidery techniques takes advantage of stitching the desired graphical patterns using a variety of textile fiber yarns and filaments.<sup>22</sup> The present prototype is comprised of conductive yarn-based interdigitated electrodes and hygroscopic adsorbent threads fabricated using embroidery additive manufacturing techniques on a face mask made from nonwoven polypropylene. Humidity sensors developed using different moisture-sensitive materials, interdigitated electrode patterns, and different substrates have been reported to impact the development and performance of the wearable devices for multiple applications. Table 1 summarizes recently reported humidity sensors comprised of diverse components and configurations. In light of the COVID-19 pandemic, several efforts have been put forward to create face-mask-embedded sensors for the detection of breath biomarkers;<sup>23,24</sup> however, they are mostly based on FFP2 (filtering face-piece 2) masks which need to be optimized for their reusability, long-term wearability, comfort, design, and performance.<sup>25–29</sup> This work takes an initiative to utilize single-use nonwoven face masks which are of low weight and with high porosity, presenting an ultimate example of a textile-based wearable device providing a high level of comfort to the wearer in addition to having good sensing capabilities toward moisture detection.

To create the interdigitated textile electrodes on the face mask, silver-plated polyamide thread was chosen to be stitched as an interdigitated pattern directly on the face mask, whereas two different types of polyester threads were embroidered and incorporated as hygroscopic sensing material between them. While there are a few reports on thread-based sensing applications for human perspiration<sup>30</sup> and temperature,<sup>31</sup>

humidity sensors are rarely reported.<sup>8</sup> Recently, the fabrication of a copper wire and a sensitive yarn-based capacitive humidity sensor fabricated by a mechanical wrapping machine has been reported.<sup>8</sup> Moreover, cotton threads have been used for humidity monitoring; however, the fabrication technology was based on the roll to roll method to coat the threads with carbon nanotube (CNT) ink.<sup>31</sup> Linen and cotton-based textile materials are reportedly used for humidity sensing coated with a metal–organic framework (MOF).<sup>11</sup> Threads used in the present work involved a facile method of sensor fabrication without any need for its functionalization with nanomaterials, thus avoiding the possible loss of nanomaterials under high humidity conditions and preventing the potential errors in generating signal consistency and sensor performance towards humidity sensing. The configuration and number of fingers of the electrodes stayed uniform for both of the embroidered sensors. The present face mask sensors relied on the variation in the dielectric permittivity of the sensitive polyester hygroscopic threads placed at the electrodes, causing the changes in capacitance.

Herein, we report a face-mask-based embroidered humidity sensor with high sensitivity towards water. The embroidery method for the fabrication of the prototype showed the ability to create robust, stable, and reliable humidity sensors with customized electrode configurations. The paper presents the proof-of-concept of using polyester-based embroidered threads as sensing material and a comparison of their performances toward capacitive humidity measurements. Furthermore, the current work marks a significant development in fabricating humidity sensors on protective face masks using an embroidery technique. The presented sensor design and prototype are well suited to be embedded into a face mask utilized for real-time monitoring of human respiration and in a significantly noninvasive way. The presence of water molecules in breathing air is a key factor to making our prepared sensor a best fit for this application as the face mask can be easily worn for a considerable period of time and can touch to breath air directly to analyze the moisture variation around the mouth and nose. The humidity sensor presents a state-of-the-art strategy which can transmit electric signals during inhalation and exhalation. As a person breathes out, the airflow reaches the sensor, resulting in the increment of RH immediately, while during breathing in, the dry air comes to the sensor, thereby generating a series of respiratory signals where an alarm can be set based on health anomalies which impact the signal such as a straight line or abnormal signal level. Thus, detection of human breath and the humidity which arises during respiration are important variables for early disease monitoring.

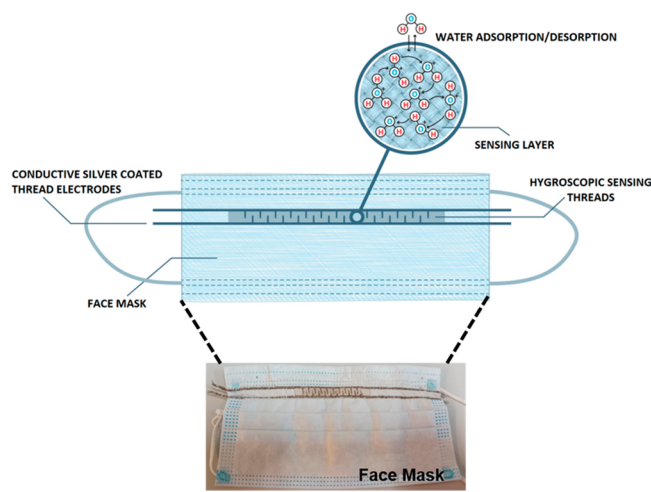
Moreover, the present piece of work manifests polymer-core-based textile threads as a novel applied material to develop a face-mask-based humidity sensor prototype which can be useful to detect exhaled breath condensate (EBC) which contains saturated levels of water. Illustration of the embroidered sensor on a single-use face mask for humidity sensing is shown in Scheme 1.

## 2. EXPERIMENTAL SECTION

### 2.1. Materials and Fabrication of Face-Mask-Based Humidity Sensors.

To fabricate the capacitive sensor, initially an interdigitated finger design was chosen, which is one of the most commonly used designs in the creation of planar capacitors.<sup>32</sup> Additional designs have been explored in the literature, such as a mixture of meandered and

**Scheme 1.** Representation of an Embroidered Humidity Sensor on a Single-Use Face Mask Comprised of Silver-Coated Conductive Polyamide Thread As an Interdigitated Electrode and Hygroscopic Polyester Threads As Sensing Material



interdigitated finger capacitors,<sup>33</sup> but the IDE structure is relatively easier to manufacture and studied in-depth and simulated,<sup>34,35</sup> which given the constraints of technical embroidery materials and mask/face morphology was a necessary compromise versus the aforementioned mixed geometry type work. The novelty of our approach is in the embroidering of the textile threads directly on the protective face mask in the form of IDE, resulting in a lightweight and natural design, minimally changing the original design of the mask. The specification in the context of dimensions and length of the fingers was adjusted to the dimension of one stripe of the commercial face mask. The design was created in AutoCAD 2021 (Autodesk, USA). The dimensions of the sensor structure are selected based on the following: (a) to be manufactured on one of the three prefabricated folds of the three-layer single use fabric/cloth face mask and (b) to be located near the position of one's nose when the mask is in use. The final design was as follows: Two busbars on the top and bottom were embroidered, with a thickness of 1.5 mm and with length slightly overshooting the mask ends, in order to accommodate for the attachment of additional electronics or instruments. Amounts of ten 0.5 mm thick fingers were attached to each busbar, with a 4.5 mm spacing between two consecutive fingers. The length of each finger was 5 mm, and the spacing between the two busbars was 6.5 mm. For the interdigitation to occur, the center of each finger of the bottom busbar was aligned with the center of the finger spacing of the top busbar. The vector drawing file was then subsequently imported to the proprietary software of the technical embroidery machine manufacturer, in order to be digitized into stitches. The design was embroidered using an industrial technical embroidery machine (JCZA 0109-550, ZSK Germany). To embroider the design, three out of the nine available standard embroidery needles were utilized, each one tensioned appropriately and terminated to the correct needle for each of the threads used.

The interdigitated fingers were embroidered using a conductive thread, particularly the Silver-Tech 150 by AMANN, which is a silver-coated polyamide thread with a nominal electrical resistance of less than 300  $\Omega$ /m. To fill the

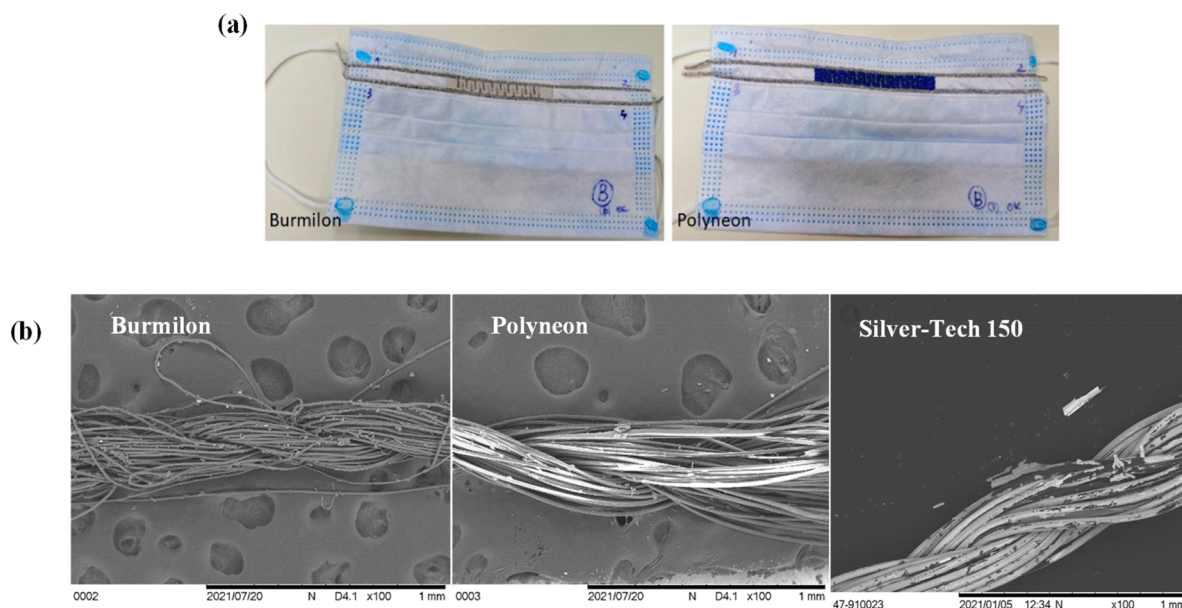


**Figure 1.** (a) Design of face mask sensors with interdigitated conductive silver-coated polyamide yarn electrodes and Burmilon and Polyneon threads as humidity-sensitive material fabricated using embroidery and (b) SEM images of threads.

gap between the two sets of fingers, two different threads were utilized, creating two different mask design variations: Burmilon #200 weight and Polyneon #60 weight by Madeira, both being polyester based (Figure 1a). SEM micrographs of implemented textile threads are presented in Figure 1b. To stabilize the masks on the embroidery frame, a tear-away water-soluble poly(vinyl-alcohol) (PVA) backing was used, which was removed at the end of the embroidery.

The main driver of selecting the design was the mask functionality. Since the embroidery technique bridges two threads, one from the top and one from the bottom of the fabric, any attempt to cross any of the three folds of the mask with the sensor would render it useless, as it would not be able to fully deploy on the face of the user. Additionally, the embroidered sensor interfacing should be done at the mask borders, to allow for easy connection to the readout electronics circuitry, and the design should be to the extent possible symmetric to avoid any parasitic and triboelectric phenomena.

## 2.2. Capacitive Measurement of the Face-Mask-Based Humidity Sensor and Surface Characterization.

For humidity sensing, the embroidered face mask sensors were set up in a self-assembled glass-sealed bottle chamber where the dielectric polyester threads were exposed to water vapors at constant temperature ( $\sim 25$  °C). Our aim was to develop a sensor capable of detecting the actual humidity changes, and for that purpose, we had to provide controlled environmental conditions at the initial stage. RH was varied to measure their sensitivity to humidity using the Owlstone system (V-OVG, Owlstone Ltd., Cambridge, UK), depicted in Supporting Information (SI) Figure S1, with controlled input and output wet airflow during which water vapors were adsorbed by the hygroscopic threads embedded between the interdigitated silver electrodes.

RH was varied slowly in the range from 28 to 78% for Burmilon and from 36 to 74% for Polyneon face mask sensors, and the corresponding change in the capacitance of the face mask sensor was measured in situ using a chemical impedance analyzer (IM3590, Hioki, Japan), also shown in Figure S1, in the frequency range from 1 Hz to 100 kHz. The difference in

the varying humidity range for both masks is due the higher sensitivity of the Burmilon thread toward water molecules which is discussed in the later sections. The complete experimental setup for humidity sensing is shown in Figure S1. The embroidered conductive thread electrodes on the face mask sensor were connected with the two wires of the test setup, which were further connected to the impedance analyzer.

The surface morphology of the conductive silver-coated polyamide yarn Silver-Tech 150 and polyester-based Burmilon and Polyneon threads was investigated by scanning electron microscopy (TM3030, Hitachi, Japan) at an accelerating voltage of 10 kV (Figure 1b). The SEM images of both polyester threads involve significant numbers of long and twisted surface channels within the thread loop which supported adsorption and transport of water molecules through them. Furthermore, the undulating surface morphology of Burmilon and Polyneon threads can be attributed to the knitting or weaving of multiple independent fibers together in a three-dimensional configuration. Moreover, the micrographic image of Silver-Tech 150 shows the similar long fibers in a continuous pattern. Moreover, Fourier transform infrared (FTIR) spectra of sensing threads Burmilon and Polyneon are shown in Figure 2 and were carried out in the spectrum range  $400\text{--}4000\text{ cm}^{-1}$  (attenuated total reflectance mode) using ALPHA (Bruker, Germany).

## 3. RESULTS AND DISCUSSION

### 3.1. Strategy of the Humidity Response Mechanism.

For a capacitive humidity sensor, the capacitance is dependent on the permittivity of the dielectric material. In the present case, under increased humidity conditions, the permittivity of water, which is relatively high, caused the permittivity of the hygroscopic threads to increase, and subsequently RH was monitored by measuring the increase in capacitance of the sensor. It is important to emphasize that Burmilon and Polyneon threads are carefully chosen as dielectric sensing material since, being polyester-based, they can adsorb moisture more easily. That is because of the presence of abundant polar

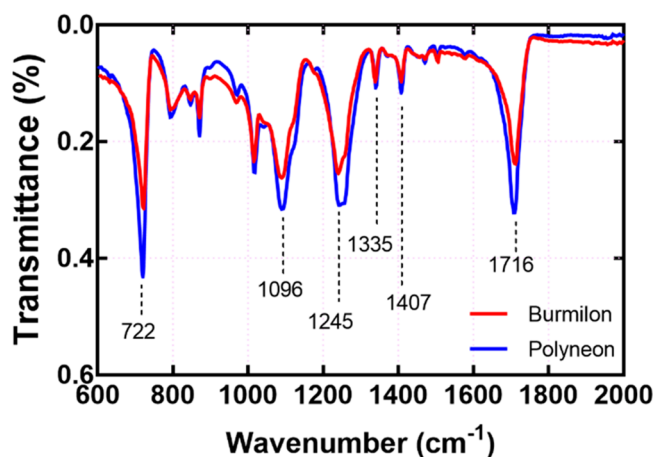


Figure 2. FTIR spectra of polyester-core-based Burmilon and Polyneon threads.

carbonyl groups on the surface of polyester fibers which can also be analyzed by FTIR spectra of threads (Figure 2) presented at  $1716\text{ cm}^{-1}$  due to the stretching vibrations of C=O groups.<sup>8</sup> The threads interact with water molecules readily through van der Waals forces, which are in principle dipole–dipole interactions. In the present work, the embroidered face mask sensor represents a capacitance-type humidity sensor, and the capacitance ( $C$ ) of the sensor is defined by  $C = \epsilon A / 4\pi kd$  where  $\epsilon$  represents the permittivity of the dielectric;  $A$  is the electrode surface area;  $k$  is the electrostatic force constant; and  $d$  represents the thickness of the dielectric. Given that  $A$  and  $d$  are constant,  $C$  is directly proportional to  $\epsilon$ .<sup>36–39</sup> The dielectric permittivity of polymer materials is reportedly much smaller than water,<sup>8</sup> allowing the permittivity of the hygroscopic threads to increase when they come into contact with water molecules. Therefore, the capacitance of the humidity sensor increases along with an increase in humidity.<sup>36,37</sup>

**3.2. Humidity-Sensing Performance of the Embroidered Face Mask Sensors.** In order to understand the capacitive behavior of the embroidered interdigitated finger-based face mask sensor toward humidity, we compared the performance of the two embroidered sensors made up of Burmilon and Polyneon threads as a sensing layer between interdigitated silver electrodes fabricated independently. With the aim to obtain the actual response of the sensor and to exclude the impact of the connecting wires, we first measured the short-circuited impedance of the connecting wires in the whole frequency range. These values were subtracted from

measured impedance obtained with the attached sensors. In this case, both embroidered sensors manifested a similar trend of change in capacitive behavior in the presence of water under different relative humidity levels in the frequency range from 1 Hz to 100 kHz. Figure 3a and Figure 3b reveals the capacitance–frequency characteristics of the Burmilon- and Polyneon-based interdigitated face mask sensors, respectively.

The RH level ranges from 28% to 78% for the Burmilon-based face mask sensor, while it ranges from 36% to 74% for the Polyneon-based sensor. It was found that the capacitance values of the sensors decreased gradually with an increase in frequency and stabilized in the higher-frequency region. The reason for this behavior might be the fact that polarization of water molecules was quite slow with the change in electric field at higher operating frequencies, which caused the permittivity of the sensing layers to remain low which eventually led to a decrease in the capacitance of the sensors.<sup>6,40–42</sup> The observed results were found in good agreement with previously reported capacitive humidity sensors, showing a similar trend.<sup>40,41</sup> Furthermore, it is clear from the logarithmic scaled graphs in Figure 3 that the capacitance of the sensors showed a linear decrease with an increase in frequency when humidity levels were above 65% in the case of Burmilon- and above 64% in the case of Polyneon-based sensors. Moreover, the results justify the utilization of our fabricated face mask prototype as an efficient humidity sensor.

In another set of developments, our embroidered face mask sensors showed a linear increase in capacitance values with an increase in different RH values. The reason for this behavior was the increase in the dielectric permittivity of the sensing textile threads, which was proportional with the increase in humidity and caused an increase in the overall sensor capacitance. As can be seen from Figure S2 (SI), the rate of change in capacitance of both the face mask sensors with increasing % RH values was found to be very high at the lower frequency of 100 Hz (Figure S2a,b). However, with an increase in frequency (Figure S2c,d), the capacitance change relatively decreased at 1, 10, and 100 kHz, respectively, which remained very low and stable compared to lower frequencies. The reason for this small variation in capacitance at higher frequencies was due to the rapid change in the electric field, which could not allow water molecules to be polarized and adsorbed by the sensing threads. In other words, polarization of water is less accelerated at higher frequencies as a result of which less electrostatic forces come into action between the sensing layer and water molecules. The basic reason behind this phenomenon is the decrease in permittivity of the sensing layer at higher frequencies,<sup>42</sup> which resulted in the reduction of

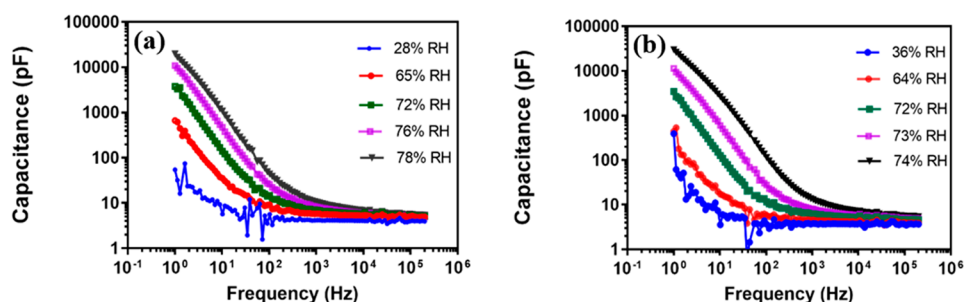
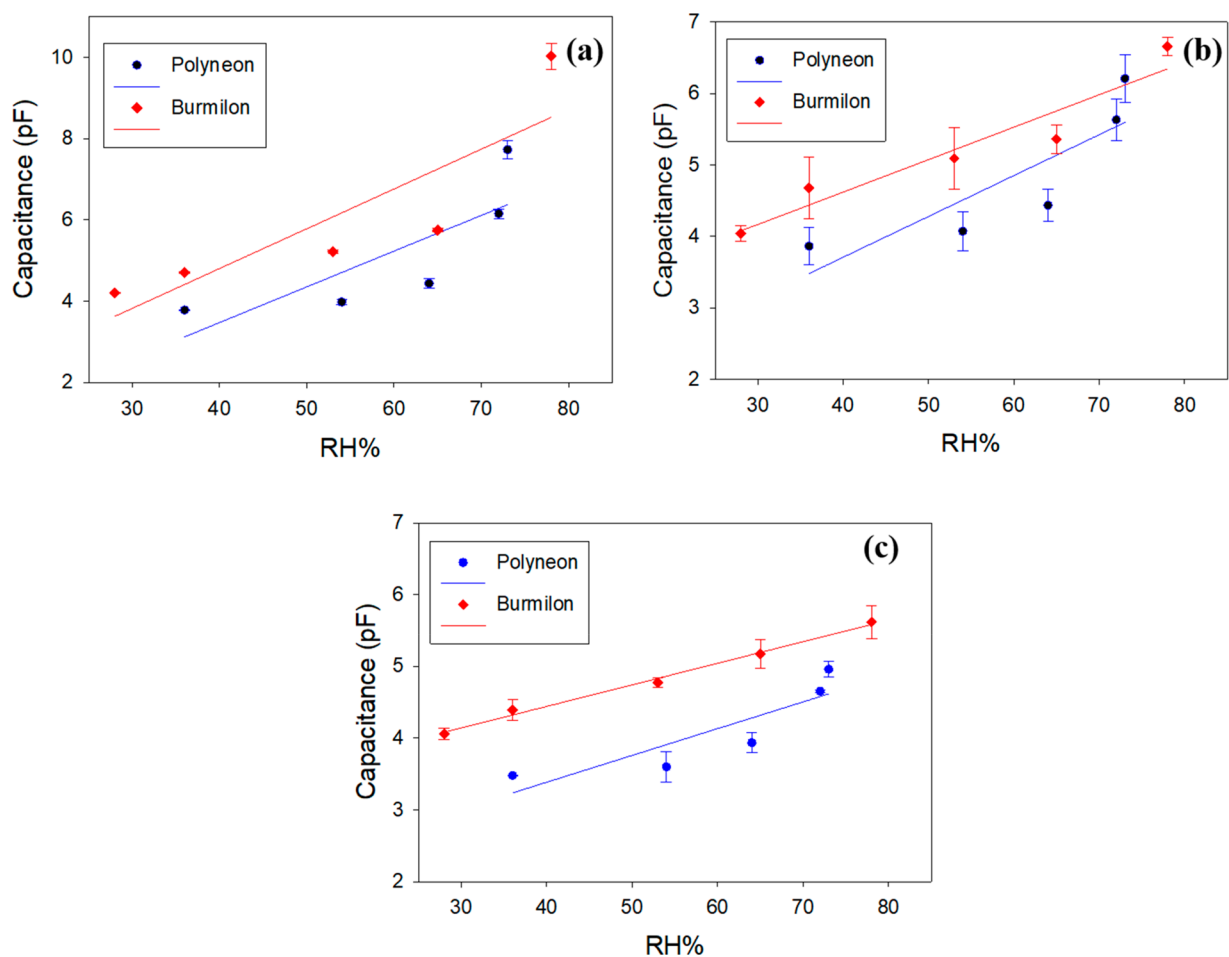


Figure 3. Trend of capacitance decrement of (a) Burmilon- and (b) Polyneon-based face mask sensors with an increase in the operating frequency range from 1 Hz to 100 kHz.



**Figure 4.** Comparison of the trend of Burmilon and Polyneon face mask humidity sensors towards a change in capacitance with respect to an increase in % RH levels at (a) 1 kHz, (b) 10 kHz, and (c) 100 kHz.

the dielectric properties of the sensing threads. Thus, a decrement in the capacitance of the sensors was observed. The results obtained showed a trend similar to other reported capacitive humidity sensors,<sup>43–46</sup> which verified good sensing performances of our embroidered face mask sensors towards humidity measurements. In addition, a Burmilon-based sensor showed a relatively good linear fit and thus high sensing performance towards capacitive humidity sensing at different frequencies in the % RH range from 28 to 78% compared to a Polyneon-based sensor where % RH was varied from 36 to 74%.

Figure 4 reveals the comparison of the linear increment of capacitance with increasing values of different % RH levels for the two embroidered face mask sensors at different frequencies of 1, 10, and 100 kHz. The obtained data for both the sensors are compiled in Table 2 which justified better performance of a Burmilon-thread-based face mask sensor. Even though the sensor responses at 1 kHz (Figure 4a) showed acceptable

**Table 2.** Comparison of Regression Datat ( $R^2$ ) of Embroidered Interdigitated Face Mask Sensors for Linear Increment of Capacitance with Increasing % RH

face mask sensor	$R^2$ at 1 kHz	$R^2$ at 10 kHz	$R^2$ at 100 kHz	% RH range
Burmilon	0.74	0.91	0.99	28–78%
Polyneon	0.63	0.72	0.76	36–74%

linearity ( $R^2 > 0.7$ ), there exist methods that can improve the linearity of the sensor response such as the piecewise linearization method which can be implemented in software or through the readout electronic hardware part. Despite the fact that the surface of the Burmilon thread is not continuous, as can be seen from the SEM image (Figure 1b), it was found to be more sensitive to water vapors than Polyneon which could be explained on the basis of the more synergistic effects into action between the conducting silver yarn electrodes and the thread itself. Moreover, at 1 kHz, the capacitance values of this sensor increased from 4.20 to 10 pF when changing the % RH from 28 to 78%, while it was increased from 3.81 to 7.73 pF in the case of a Polyneon face mask sensor when increasing the % RH from 36 to 74%. However, at 10 kHz, for the Burmilon sensor, the capacitance values increased from 4.04 to 6.66 pF, and at 100 kHz, they increased from 4.06 to 5.62 pF. Likewise, at 10 kHz, the Polyneon-based sensor showed an increment of capacitance from 3.86 to 6.21 pF, while it changed from 3.49 to 4.96 pF at 100 kHz when varying the humidity conditions. The observed results justified the small linear change in capacitance with increasing % RH in the high-frequency region. The capacitance values reported represent the mean values of the three measurements performed in each case. The limit of detection (LOD) values for the proposed sensor at different frequencies are presented in Table 3. The LOD values are calculated using the formula  $3 \times \text{SD}/S$  derived from a linear regression equation where SD is the standard

**Table 3. Limit of Detection (LOD in % RH) Values of Face Mask Sensors Towards Humidity Detection at Different Frequencies**

face mask sensor	LOD at 1 kHz	LOD at 10 kHz	LOD at 100 kHz
Burmilon	27.41	19.37	11.46
Polyneon	38.65	34.42	29.79

deviation of the intercept and  $S$  is the slope from the regression data.

In the next step of our experiment, the hysteresis characteristics of the embroidered face mask sensors were analyzed by performing adsorption and desorption cycles at 100 kHz. The capacitance of the sensors was recorded at each humidity level in the range from 36 to 78% and back in the case of a Burmilon-based face mask sensor, while % RH was varied from 36 to 74% and back in the case of a Polyneon-based face mask sensor. Figure S3 (SI) shows the adsorption and desorption properties of the sensors with hysteresis which justifies the fact that face mask sensors readily adsorb moisture, while the recovery time and desorption process are low. The performance of a Burmilon-based sensor was better due to less hysteresis at lower humidity levels during adsorption and desorption processes.

**3.3. Sensitivity, Stability, and Repeatability of the Embroidered Face Mask Humidity Sensors.** As the next segment of our research related to the evaluation of the sensing performance of the proposed embroidered face mask sensors, sensitivity toward humidity was calculated using the equation  $S = \Delta C / \Delta RH$  where  $\Delta C$  represents the change in capacitance response of the sensor, whereas  $\Delta RH$  is the change of RH values observed by the sensor. Figure 5a and Figure 5b shows the humidity sensitivity comparison of the two embroidered face mask capacitive sensors at 1 and 100 kHz, respectively. The results showed higher sensitivity of the Burmilon-based interdigitated face mask sensor than the Polyneon sensor toward humidity measurements. The high sensitivity of the Burmilon-based face mask capacitive sensor (0.116 at 1 kHz and 0.052 at 100 kHz) than the Polyneon sensor (0.107 at 1 kHz and 0.039 at 100 kHz) is justified in all the previous data provided in this paper, which probably can be attributed to a larger number of surface polar groups on the fiber which facilitate ion transport and thus adsorption of moisture under different humidity conditions.

Moreover, Figure 6 corresponds to the stability studies of embroidered face mask sensors toward humidity. Figure 6a and

6b presents the relative data of the fabricated Burmilon- and Polyneon-based face mask sensors, respectively, at 1 kHz under different humidity levels. Figure 6c and Figure 6d compares the sensing characteristics of the two sensors at 10 kHz, while Figure 6e and 6f reports them at 100 kHz. The capacitance values were measured three times over a period of 20 min at each humidity level for each sensor independently at different time intervals. The capacitive response of the embroidered face mask humidity sensors was found to be stable and reproducible with each measurement under different % RH conditions of 52% and 70% in the case of the Burmilon-based sensor and under 58% and 70% humidity conditions in the case of the Polyneon-based sensor. The change observed in the humidity conditions for both sensors was due to the impact of wet airflow which increased the water adsorption to 58% RH in the case of Polyneon. Both face mask sensors demonstrated good stability toward humidity sensing with acceptable relative standard deviations % RSD = 1.15–6.06 for the Burmilon and % RSD = 1.95–5.24 for the Polyneon sensors, respectively at different frequencies. In a recent example of textile-based humidity sensors, linen and cotton materials were tested toward moisture detection and their reproducibility at around 19% RH for 160 min.<sup>11</sup> However, in the present case, the reason for choosing 20 min and high RH values for this study was due to the fact that this time frame was able enough for stable and repeatable measurement of capacitance at different RH levels.

In addition, the dynamic response of the face mask sensors was further evaluated by tracking the capacitance of the face mask sensors at different % RH levels over the span of 80 min at 10 kHz and at an operating potential of 0.1 V. The sensors demonstrated an increment in capacitance values with an increase in humidity conditions while being stable at each humidity level for 20 min. The capacitive response characteristics of the embroidered face mask sensors towards humidity measurements are shown in Figure 7, justifying repeatable performances.

**3.4. Real-Time Sensing Properties of Fabricated Face Mask Sensors.** Real-time properties of the fabricated face mask sensor were determined using the Burmilon-based sensor, considering its better sensing performance. Respiration rate monitoring of two healthy male volunteers was performed. Hioki IM3590 was connected to the laptop with installed control software (LCR Meter Sample Application ver. 1.3.4.0) provided by the Hioki, available at the official Web site.<sup>47</sup>

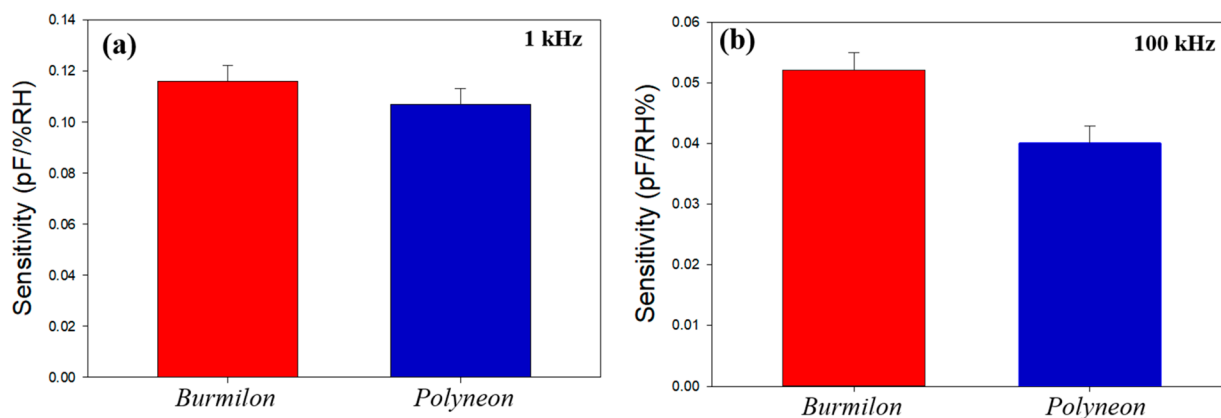


**Figure 5.** Sensitivity comparison of embroidered face mask sensors at (a) 1 kHz and (b) at 100 kHz.

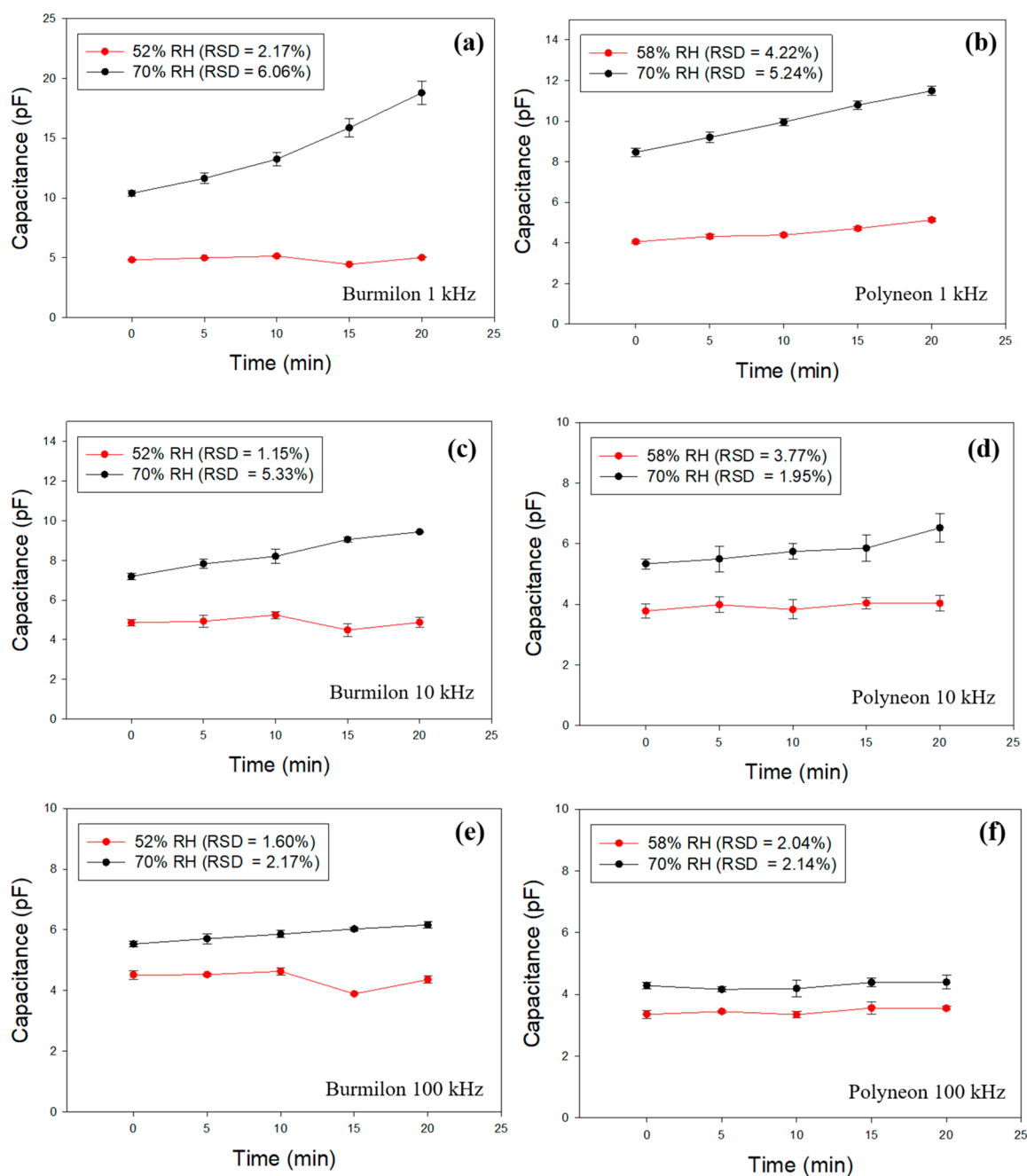


**Figure 6.** Stability data of Burmilon and Polyneon face mask sensors at different frequencies: (a) and (b) at 1 kHz, (c) and (d) at 10 kHz, (e) and (f) at 100 kHz with acceptable % RSD values.

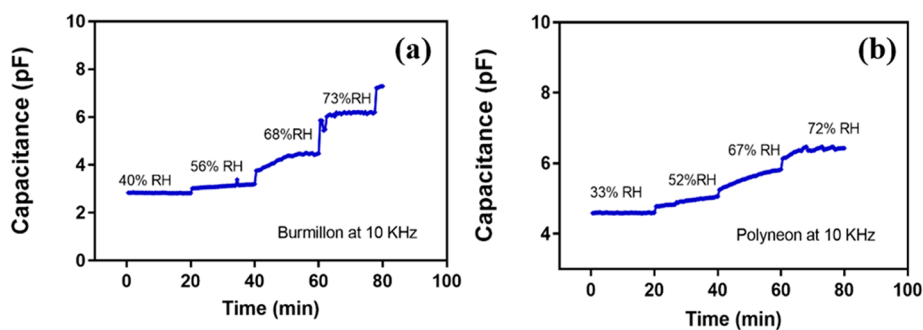


**Figure 7.** Capacitive response of (a) Burmilon and (b) Polyneon face mask sensors showing dynamic response evaluated for 20 min at each humidity level at 10 kHz.

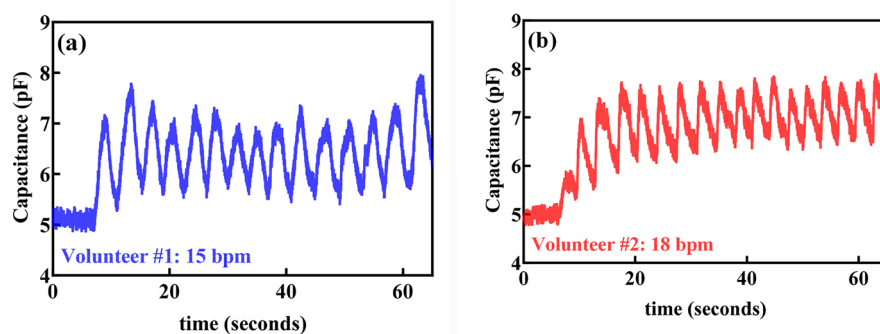


Figure 8. Capacitive response of face mask sensors for (a) volunteer 1 and (b) volunteer 2 during respiration rate monitoring.

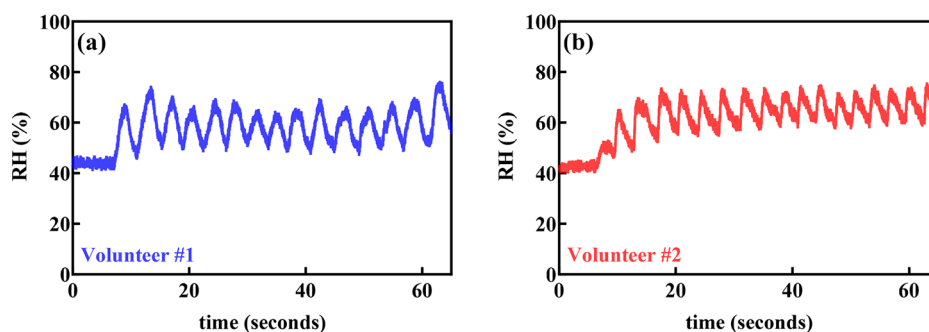


Figure 9. Observed % relative humidity changes during human respiration of (a) volunteer 1 and (b) volunteer 2.

Capacitance data sampling was performed 90 times per second at a testing frequency of 1 kHz. All volunteers signed informed consents before the data acquisition. Volunteers were initially instructed to sit and to rest for about 2 min. Data recording started with an initial few seconds of breath holding, which was followed by normal breathing for one minute. The respiration rate (breaths per minute (bpm)) was confirmed by physical assessment (counting by the subject as well as the supervising researcher). As can be seen from Figure 8, the breathing rates (of 15 and 18 bpm) were successfully registered.

Respiration rates from 12 to 20 bpm are in general considered as common for healthy adults.<sup>37</sup> It is clear from Figure 8 that the obtained respiration rates with our sensor (15 bpm and 18 bpm) are in the expected range, as there are other reported ranges of 19 bpm<sup>36</sup> and 17 bpm.<sup>39</sup> Using the equation for the linear fit (Figure 4) at 1 kHz,  $Y = 0.08865X + 1.211$  (where  $X$  is relative humidity in % and  $Y$  is capacitance in pF), and taking into consideration the measured values as shown in Figure 8, the obtained relative humidity changes during the human respiration are shown in Figure 9 which shows the utility of our prepared sensor for practical applications of respiration monitoring.

**3.5. Study of Washability.** Washing studies of the face mask sensors were performed in the absence of humidity conditions. The capacitance of the Burmilon-based face mask sensor was recorded at normal room conditions and then compared with the capacitance obtained after its washing (Figure S4, SI). Washing of the face mask sensor was performed using lukewarm water at a recorded temperature of 35 °C followed by drying at room temperature. The process was followed three times, and the performance of the sensor was recorded in an ambient atmosphere. The idea behind washing the sensor was to relate its humidity sensing performance and reusability after wetting and drying in normal

atmospheric conditions. The results clearly reveal a slow but steady decrease in its capacitance with an increase in frequency. However, a nominal decrease in its capacitance values was observed after its washing. The baseline capacitance values without humidity conditions at 1, 10, and 100 kHz were measured as 3.59 pF, 3.50 pF, and 3.46 pF, respectively, which, however, after washing decreased to 3.29 pF, 2.71 pF, and 2.3 pF. The observed results manifested that there was no significant change in the capacitance values of the interdigitated face mask sensor even after washing, and the electrical properties of the conductive silver-coated polyamide yarn remained intact. The study motivated the use of textile-based conductive threads to fabricate electrical sensors for various applications. Further, it was justified that the fabricated face mask could be applied for use in normal environmental conditions.

## 4. CONCLUSIONS

This paper aimed to develop an innovative design of a humidity sensor based on textile threads embroidered on face masks as substrates. The methodology employed to fabricate the sensor took advantage of the high conducting nature of silver-coated polyamide threads to embroider interdigitated electrodes and polyester-based hygroscopic threads, which responded to the change in moisture levels by changing the dielectric and permittivity properties of the embroidered design which acted as a capacitor. Individual performances of interdigitated finger face mask sensors filled with different polyester threads were evaluated and then compared to their ability to detect water molecules under different humidity conditions. The study presents the first use of polyester threads as embroidered dielectric sensing material for moisture detection, using face mask as a substrate. High sensitivity and capacitive trends of embroidered interdigitated face mask

sensors in the present paper were found in accordance with the literature and with the proof-of-concept capacitive humidity measurements. The present work successfully demonstrated potential utilization of the embroidered face mask sensor in various humidity-monitoring applications, including human respiration (breathing rate and relative humidity changes). It also opened new avenues to develop several other textile sensors using sensitive fibers and substrates. Additionally, the proposed idea can be used on recycled textile face masks, giving them new useful roles and protecting our environment as well. The presented face mask prototype will be applied to detect volatile organic compounds (VOCs) in our future work.

## ■ ASSOCIATED CONTENT

### SI Supporting Information

The Supporting Information is available free of charge at <https://pubs.acs.org/doi/10.1021/acsomega.2c05162>.

Figures: experimental setup used for humidity measurement, linear fitting curves of Burmilon and Polyneon interdigitated electrode-based face mask sensors with increasing % RH levels at different frequencies, hysteresis characteristics of face mask sensors, and washing properties of Burmilon-based face mask sensors (PDF)

## ■ AUTHOR INFORMATION

### Corresponding Author

Ankita Sinha – University of Novi Sad, Faculty of Technical Sciences, 21000 Novi Sad, Serbia; [orcid.org/0000-0002-8842-0098](https://orcid.org/0000-0002-8842-0098); Email: [ankitasinha11@outlook.com](mailto:ankitasinha11@outlook.com)

### Authors

Adrian K. Stavrakis – University of Novi Sad, Faculty of Technical Sciences, 21000 Novi Sad, Serbia

Mitar Simić – University of Novi Sad, Faculty of Technical Sciences, 21000 Novi Sad, Serbia; [orcid.org/0000-0002-8300-022X](https://orcid.org/0000-0002-8300-022X)

Goran M. Stojanović – University of Novi Sad, Faculty of Technical Sciences, 21000 Novi Sad, Serbia

Complete contact information is available at:

<https://pubs.acs.org/10.1021/acsomega.2c05162>

### Author Contributions

<sup>‡</sup>A.S. and A.K.S. contributed equally to this work. A.S.: Data curation, Formal analysis, Investigation, Validation, Writing—original draft, review, and editing. A.K.S.: Data curation, Formal analysis, Software, Visualization, Writing—original draft, review, and editing. M.S.: Formal analysis, Writing—review and editing. G.M.S.: Conceptualization, Funding acquisition, Methodology, Project administration, Resources, Supervision, Writing—review and editing.

### Notes

The authors declare no competing financial interest.

## ■ ACKNOWLEDGMENTS

This study is supported by the European Union's Horizon 2020 research and innovation program under grant agreement no. 854194.

## ■ REFERENCES

- (1) Delipinar, T.; Shafique, A.; Gohar, M. S.; Yapici, M. K. Fabrication and materials integration of flexible humidity sensors for emerging applications. *ACS Omega* **2021**, *6*, 8744–8753.
- (2) Wang, Y.; Huang, J. Recent advancements in flexible humidity sensors. *J. Semicond.* **2020**, *41*, 040401.
- (3) Singh, E.; Meyyappan, M.; Nalwa, H. S. Flexible Graphene-Based Wearable Gas and Chemical Sensors. *ACS Appl. Mater. Interfaces* **2017**, *9*, 34544–34586.
- (4) Krishnan, S. K.; Singh, E.; Singh, P.; Meyyappan, M.; Nalwa, H. S. A review on graphene-based nanocomposites for electrochemical and fluorescent biosensors. *RSC Adv.* **2019**, *9*, 8778–8881.
- (5) Duan, Z.; Jiang, Y.; Tai, H. Recent advances in humidity sensors for human body-related humidity detection. *J. Mater. Chem. C* **2021**, *9*, 14963–14980.
- (6) Guntner, A. T.; Abegg, S.; Konigstein, K.; Gerber, P. A.; Schmidt-Trucksass, A.; Pratsinis, S. E. Breath Sensors for Health Monitoring. *ACS Sens.* **2019**, *4*, 268–280.
- (7) Tai, H.; Duan, Z.; Wang, Y.; Wang, S.; Jiang, Y. Paper based sensors for gas, humidity, and strain detections: a review. *ACS Appl. Mater. Interfaces* **2020**, *12*, 31037–31053.
- (8) Ma, L.; Wu, R.; Patil, A.; Zhu, S.; Meng, Z.; Meng, H.; Hou, C.; Zhang, Y.; Liu, Q.; Yu, R.; Wang, J.; Lin, N.; Liu, X. Y. Full-textile wireless flexible humidity sensor for human physiological monitoring. *Adv. Funct. Mater.* **2019**, *29*, 1904549.
- (9) Kojić, T.; Stojanović, G. M.; Miletić, A.; Radovanović, M.; Al-Salami, H.; Arduini, F. Testing and characterization of different papers as substrate material for printed electronics and application in humidity sensor. *Sensors Mater.* **2019**, *31*, 2981–2995.
- (10) Kinkeldei, T.; Mattana, G.; Leuenberger, D.; Ataman, C.; Lopez, F. M.; Quintero, A. V.; Briand, D.; Nisato, G.; Rooij, N. F.; Tröster, G. Feasibility of printing woven humidity and temperature sensors for the integration into electronic textiles. *Adv. Sci. Technol.* **2012**, *80*, 77–82.
- (11) Rauf, S.; Vijjapu, M. T.; Andrés, M. A.; Gascón, I.; Roubeau, O.; Eddaoudi, M.; Salama, K. N. Highly selective metal-organic framework textile humidity sensor. *ACS Appl. Mater. Interfaces* **2020**, *12*, 29999–30006.
- (12) Shim, B. S.; Chen, W.; Doty, C.; Xu, C.; Kotov, N. A. Smart electronic yarns and wearable fabrics for human biomonitoring made by carbon nanotube coating with polyelectrolytes. *Nano Lett.* **2008**, *8*, 4151–4157.
- (13) Zhou, G.; Byun, J. H.; Oh, Jung, B. M.; Cha, H. J.; Seong, D. G.; Um, M. K.; Hyun, S.; Chou, T. W. Highly sensitive wearable textile-based humidity sensor made of high-strength, single-walled carbon nanotube/poly(vinyl alcohol) filaments. *ACS Appl. Mater. Interfaces* **2017**, *9*, 4788–4797.
- (14) Weremczuk, J.; Tarapata, G.; Jachowicz, R. Humidity sensor printed on textile with use of ink-jet technology. *Procedia Eng.* **2012**, *47*, 1366–1369.
- (15) McColl, D.; Cartlidge, B.; Connolly, P. Real-time monitoring of moisture levels in wound dressings in vitro: an experimental study. *Int. J. Surg.* **2007**, *5*, 316–322.
- (16) Mattana, G.; Kinkeldei, T.; Leuenberger, D.; Ataman, C.; Ruan, J. J.; Molina-Lopez, F.; Quintero, A. V.; Nisato, G.; Troster, G.; Briand, D.; de Rooij, N. F. Woven temperature and humidity sensors on flexible plastic substrates for e-textile applications. *IEEE Sens.* **2013**, *13*, 3901–3909.
- (17) Wang, L.; Wang, L.; Zhang, Y.; Pan, J.; Li, S.; Sun, X.; Zhang, B.; Peng, H. Weaving sensing fibers into electrochemical fabric for real-time health monitoring. *Adv. Funct. Mater.* **2018**, *28*, 1804456.
- (18) Kubiak, P.; Lesnikowski, J.; Gniotek, K. Textile sweat sensor for underwear convenience measurement. *Fibres Text. East. Eur.* **2016**, *24*, 151–155.
- (19) Guo, Y. N.; Gao, Z. Y.; Wang, X. X.; Sun, L.; Yan, X.; Yan, S. Y.; Long, Y. Z.; Han, W. P. A highly stretchable humidity sensor based on Spandex covered yarns and nanostructured polyaniline. *RSC Adv.* **2018**, *8*, 1078–1082.

- (20) Jang, J. H.; Han, J. I. Cylindrical relative humidity sensor based on poly-vinyl alcohol (PVA) for wearable computing devices with enhanced sensitivity. *Sensors Actuators, A Phys.* **2017**, *261*, 268–273.
- (21) Komazaki, Y.; Uemura, S. Stretchable, printable, and tunable PDMS-CaCl<sub>2</sub> microcomposite for capacitive humidity sensors on textiles. *Sensors Actuators, B Chem.* **2019**, *297*, 126711.
- (22) Liu, X.; Lillehoj, P. B. Embroidered electrochemical sensors for biomolecular detection. *Lab Chip* **2016**, *16*, 2093–2098.
- (23) Escobedo, P.; Fernández-Ramos, M. D.; López-Ruiz, N.; Moyano-Rodríguez, O.; Martínez Olmos, A.; Pérez de Vargas-Sansalvador, I. M.; Carvajal, M. A.; Capitán-Vallvey, L. F.; Palma, A. J. Smart facemask for wireless CO<sub>2</sub> monitoring. *Nat. Commun.* **2022**, *13*, 72.
- (24) Tipparaju, V. V.; Xian, X.; Bridgeman, D.; Wang, D.; Tsow, F.; Forzani, E.; Tao, N. Reliable breathing tracking with wearable mask device. *IEEE Sens.* **2020**, *20*, 5510.
- (25) Geiss, O. Effect of wearing face masks on the carbon dioxide concentration in the breathing zone. *Aerosol Air Qual. Res.* **2021**, *21*, 200403.
- (26) Cherrie, J. W.; Wang, S.; Mueller, W.; Nelson, C. W.; Loh, M. In-mask temperature and humidity can validate respirator wear time and indicate lung health status. *J. Expo Sci. Environ. Epidemiol.* **2019**, *29*, 578–583.
- (27) Lu, Q.; Chen, H.; Zeng, Y.; Xue, J.; Cao, X.; Wang, N.; Wang, Z. Intelligent facemask based on triboelectric nanogenerator for respiratory monitoring. *Nano Energy* **2022**, *91*, 106612.
- (28) Schmitt, J.; Jones, L. S.; Aebly, E. A.; Gloor, C.; Moser, B.; Wang, J. Protection level and reusability of a modified full-face snorkel mask as alternative personal protective equipment for healthcare workers during the COVID-19 pandemic. *Chem. Res. Toxicol.* **2021**, *34*, 110–118.
- (29) El-Atab, N.; Qaiser, N.; Badghaish, H.; Shaikh, S. F.; Hussain, M. M. Flexible nanoporous template for the design and development of reusable anti-COVID-19 hydrophobic face masks. *ACS Nano* **2020**, *14*, 7659–7665.
- (30) Jia, J.; Xu, C.; Pan, S.; Xia, S.; Wei, P.; Noh, H. Y.; Zhang, P.; Jiang, X. Conductive thread-based textile sensor for continuous perspiration level monitoring. *Sensors* **2018**, *18*, 3775.
- (31) Hasanpour, S.; Karperien, L.; Walsh, T.; Jahanshahi, M.; Hadisi, Z.; Neale, K. J.; Christie, B. R.; Djilali, N.; Akbari, M. A hybrid thread-based temperature and humidity sensor for continuous wound monitoring. *Sens Actuators B: Chem.* **2022**, *370*, 132414.
- (32) Sathya, S.; Muruganand, S.; Manikandan, N.; Karupphasamy, K. Design of capacitance based on interdigitated electrode for BioMEMS sensor application. *Mater. Sci. Semicond Process* **2019**, *101*, 206–213.
- (33) Rivadeneyra, A.; Fernandez-Salmeron, J.; Banqueri, J.; Lopez-Villanueva, J. A.; Capitan-Vallvey, L. F.; Palma, A. J. A novel electrode structure compared with interdigitated electrodes as capacitive sensor. *Sens Actuators B: Chem.* **2014**, *204*, 552–560.
- (34) Igreja, R.; Dias, C. J. Analytical evaluation of the interdigital electrodes capacitance for a multi-layered structure. *Sens Actuators A: Phys.* **2004**, *112*, 291–301.
- (35) Mohd Syaifudin, A. R.; Mukhopadhyay, S. C.; Yu, P. L. Modelling and fabrication of optimum structure of novel interdigital sensors for food inspection. *Int. J. Numer. Model.: Electron. Netw. Devices Fields* **2012**, *25*, 64–81.
- (36) Zhang, Y.; Wu, Y.; Duan, Z.; Liu, B.; Zhao, Q.; Yuan, Z.; Li, S.; Liang, J.; Jiang, Y.; Tai, H. High performance humidity sensor based on 3D mesoporous Co<sub>3</sub>O<sub>4</sub> hollow polyhedron for multifunctional applications. *Appl. Surf. Sci.* **2022**, *585*, 152698.
- (37) Duan, Z.; Yuan, Z.; Jiang, Y.; Zhao, Q.; Huang, Q.; Zhang, Y.; Liu, B.; Tai, H. Power generation humidity sensor based on primary battery structure. *Chem. Engineer. J.* **2022**, *446*, 136910.
- (38) Duan, Z.; Jiang, Y.; Tai, H. Recent advances in humidity sensors for human body related humidity detection. *J. Mater. Chem. C* **2021**, *9*, 14963–14980.
- (39) Zhao, Q.; Jiang, Y.; Duan, Z.; Yuan, Z.; Zha, J.; Wu, Z.; Huang, Q.; Zhou, Z.; Li, H.; He, F.; Su, Y.; Tan, C.; Tai, H. A Nb<sub>2</sub>CT<sub>x</sub>/sodium alginate-based composite film with neuron-like network for self-powered humidity sensing. *Chem. Engineer. J.* **2022**, *438*, 135588.
- (40) Wang, Y.; Hou, S.; Li, T.; Jin, S.; Shao, Y.; Yang, H.; Wu, D.; Dai, S.; Lu, Y.; Chen, S.; Huang, J. Flexible capacitive humidity sensors based on ionic conductive wood-derived cellulose nanopapers. *ACS Appl. Mater. Interfaces* **2020**, *12*, 41896–41904.
- (41) Li, B.; Tian, Q.; Su, H.; Wang, X.; Wang, T.; Zhang, D. High sensitivity portable capacitive humidity sensor based on In<sub>2</sub>O<sub>3</sub> nanocubes-decorated GO nanosheets and its wearable application in respiration detection. *Sensors Actuators, B Chem.* **2019**, *299*, 126973.
- (42) McGhee, J. R.; Sagu, J. S.; Southee, D. J.; Evans, P. S. A.; Wijayantha, K. G. P. Printed, fully metal oxide, capacitive humidity sensors using conductive indium tin oxide inks. *ACS Appl. Electron. Mater.* **2020**, *2*, 3593–3600.
- (43) Shah, M.; Ahmad, Z.; Sulaiman, K.; Karimov, K. S.; Sayyad, M. H. Carbon nanotubes nanocomposite in humidity sensors. *Solid. State. Electron.* **2012**, *69*, 18–21.
- (44) Zhang, D.; Tong, J.; Xia, B.; Xue, Q. Ultrahigh performance humidity sensor based on layer-by-layer self-assembly of graphene oxide/polyelectrolyte nanocomposite film. *Sensors Actuators, B Chem.* **2014**, *203*, 263–270.
- (45) Zhang, D.; Sun, Y.; Li, P.; Zhang, Y. Facile fabrication of MoS<sub>2</sub> modified SnO<sub>2</sub> hybrid nanocomposite for ultrasensitive humidity sensing. *ACS Appl. Mater. Interfaces* **2016**, *8*, 14142–14149.
- (46) Hammouche, H.; Achour, H.; Makhlof, S.; Chaouchi, A.; Laghrouche, M. A comparative study of capacitive humidity sensor based on keratin film, keratin/graphene oxide, and keratin/carbon fibers. *Sensors Actuators, A Phys.* **2021**, *329*, 112805.
- (47) [https://www.hioki.com/global/support/download/software/versionup/detail/id\\_539](https://www.hioki.com/global/support/download/software/versionup/detail/id_539) (accessed September 1, 2022).